Correlation between the electric and acoustic signals emitted during compression of brittle materials

Ermioni D. Pasiou
National Technical University of Athens, Department of Mechanics, Laboratory for Testing and Materials, 5 Heroes of Polytechnion Avenue, Theocaris Building, 157 73, Athens, Greece
epasiou@teemail.gr

Dimos Triantis
Technological Educational Institution of Athens, Department of Electronics, Laboratory of Electronic Devices and Materials, Ag. Spiridonos Street, 122 10, Athens, Greece
triantis@teiath.gr

ABSTRACT. An experimental protocol is described including a series of uniaxial compression tests of three brittle materials (marble, mortar and glass). The Acoustic Emission (AE) technique and the Pressure Stimulated Currents (PSC) one are used since the recordings of both techniques are strongly related to the formation of cracking in brittle materials. In the present paper, the correlation of these techniques is investigated, which is finally proven to be very satisfactory.

KEYWORDS. Pressure stimulated currents (PSC); Acoustic emission (AE); Compression; Brittle materials.

Citation: Pasiou, E.D., Triantis, D., Correlation between the electric and acoustic signals emitted during compression of brittle materials, Frattura ed Integrità Strutturale, 40 (2017) 41-51.

Received: 23.12.2016
Accepted: 07.02.2017
Published: 01.04.2017

INTRODUCTION

Monitoring the mechanical response of various brittle materials under compressive loading is of great interest in a range of application fields. Especially, monitoring their damage evolution is crucial since actions can be taken in time in order to preserve the integrity of structures. In this context, a series of diagnostic methods have been developed in order to assess damage and also to detect impending failure of the materials.

Acoustic emission (AE) technique is among the as above techniques [1]. When a material is loaded, transient elastic waves are generated within the material (which are mainly depended on the material's irreversible deformations) and travel along the specimen. These waves are called acoustic emissions and they are recorded by sensors which are attached on the specimen. The first studies of acoustic emissions in geomaterials were carried out in 1938. Monitoring a specimen/structure during its whole loading history is one of the advantages of this technique since in general the increase of acoustic activity, which is observed as the specimen approaches failure, is strongly correlated to the decay of the

mechanical properties of the material. The improved b-value (Ib-value) is one of the acoustic characteristics which is related to the impending failure [1-2] since its value changes during the failure process. Ib-value, firstly introduced by Shiotani et al. [3], is defined as:

$$Ib = \frac{\log N(\mu - \alpha_1\sigma) - \log N(\mu + \alpha_2\sigma)}{(\alpha_1 + \alpha_2)\cdot\sigma} \quad (1)$$

where μ is the mean amplitude, σ the standard deviation and α_1, α_2 constants (which are usually equal to 1 [1]).
Damage process is also well detected by the Pressure Stimulated Currents (PSC) technique [4] and more specific by the weak electric signals emitted during the generation of micro-cracks in brittle materials when they are subjected to mechanical loading [5-6]. More than ten years ago, electric signals were recorded by Stavrakas et al. [6] during mechanical loading of marble. A few years later, electric signals were also recorded when specimens of rock materials and cement based materials were tested [7-10]. The signal was captured by a pair of gold plated electrodes and it was recorded using a sensitive electrometer. In all cases, when the applied stress was above 80% of the maximum stress, PSC increased rapidly reaching a maximum value just before the specimen's fracture [4, 10]. PSC technique is also used by other researchers [11-14] while similar techniques are used [15-16] to detect cracking of rocks and concrete specimens. Some of the advantages of the PSC technique are the low cost of the sensors and the easiness of sensors' production as well as the fact that electrodes don't affect the specimens' structure or the stress and strain fields.
The qualitative correlation of the aforementioned techniques has already been mentioned in previous studies during trivial tests [17-18] as well as in more complex specimens (i.e. made of more than one material [19]). In the present experimental protocol, specimens of three brittle materials (marble, mortar and glass) are subjected to uniaxial compression tests in order to confirm and quantify the correlation of PSC and AE techniques.

MATERIALS AND EXPERIMENTAL SET UP

Materials

Dionysos marble is the stone exclusively used for the restoration of the monuments of the Athenian Acropolis. Its chemical composition is 98% of calcite, 0.5% of muscovite, 0.3% of sericite, 0.2% of quartz and 0.1% of chlorite. Its grain size varies from 100 μm to 400 μm and its specific and apparent densities are equal to 2730 kg/m^3 and 2717 kg/m^3, respectively. The absorption coefficient by weight of Dionysos marble is about 0.11% and its thermal expansion coefficient is 9x10^{-6} /^{o}C between 15 ^{o}C and 100 ^{o}C. Its very low porosity varies between 0.3% (virgin state) to 0.7% (superficial porosity) [20].
The mechanical properties of Dionysos marble vary between broad limits [21]. The specific marble is of rather orthotropic nature, i.e. it is characterized by three different anisotropy directions. However, it can be approximately considered as a transversely isotropic material described adequately with the aid of five elastic constants as it was definitely concluded by detailed experimental protocols including direct tension and compression tests as well as three-point bending and Brazilian Disc tests [22-29]. The as above experimental protocols revealed also that Dionysos marble is slightly non-linear (both in the tension and in the compression regime) and slightly bimodular, i.e. the elastic modulus in compression is about 15% higher than the respective one in tension [24, 25].
Three marble specimens were used in the present study of prismatic shape with dimensions 40 mm x 40 mm x 100 mm. The load was applied normal to the material layers, i.e. along the strong direction of Dionysos marble's anisotropy.
The second material tested was a mortar which consisted of three parts of fine sand, one part of ordinary Portland cement and half part of water. The grain size of the sand varied between 3 mm to 6 mm and its fineness modulus was equal to 2.8. In addition, its specific gravity was found equal to 2.6, its density was 2200 kg/m^3 and its porosity was evaluated at approximately 8% [10].
The constituents of the mortar were mixed at a low speed to enable better moisturizing of the cement grains while at the end of the production process the mixture was agitated very fast for 1 min. Mortar was formed in three prismatic blocks using metallic moulds of dimensions 50 mm x 50 mm x 70 mm the inner surfaces of which were oiled. The moulds were mounted on a desktop vibrator in order to enable compaction. The mortar prismatic blocks were demoulded after 24 h and they were cured in a room with constant ambient temperature of 22 °C and 75-80% humidity. The specimens were stored for 100 days to reach 90-95% of their strength [30].
The third material studied in the present experimental protocol was one of the most common types of glass produced, i.e. the soda-lime-silica one (or simply soda glass). One of its most important advantages is that it is nearly chemically inert,

therefore it doesn't react with other chemicals when they come into contact with it. Soda glass in usually used to make windows, bottles, jars, vials and other laboratory equipment. The chemical composition of this type of glass is presented in Tab. 1. In the present experimental protocol three prismatic blocks (30 mm x 30 mm x 80 mm) were used.

Components	SiO_2	Al_2O_3	Na_2O	K_2O	CaO	MgO	Fe_2O_3	TiO_2	P_2O_5	ZrO_2
%	72.4	1.26	13.4	0.24	8.53	3.95	0.16	0.063	0.018	0.05

Table 1: Chemical composition of soda-lime-silica glass [31].

Experimental set up

Before testing, one Kyowa strain gauge (of 5 mm gauge length and of 120 Ω gauge resistance) was glued on the front surface of the specimen (at the middle of its height and of its width as it is seen in Fig.1a) in order to measure the axial strain during the tests. In addition, one acoustic sensor R15α (denoted by number 3 in Fig.1b) was coupled on the opposite surface of the specimen by means of silicone and one preamplifier with 40 dB gain was also used (the equipment and the software used were by Mistras Group, Inc.). Finally, a pair of electrodes was attached on the two side opposite surfaces of each specimen (orange ellipses in Fig.1a and numbers 1,2 in Fig.1b) in such a way so as the imaginary line connecting them to be perpendicular to the loading axis. A sensitive programmable electrometer (Keithley, 6517A), capable of resolving currents as low as 0.1 fA and as high as 20 mA in 11 ranges, was used to record the electric signals. It should be underlined that thin teflon plates were placed between the specimen and the loading platens for the specimen's electrical isolation. All specimens were subjected to compressive loading under load control conditions ($d\sigma/dt$=0.3 MPa/s) simulating quasi-static loading.

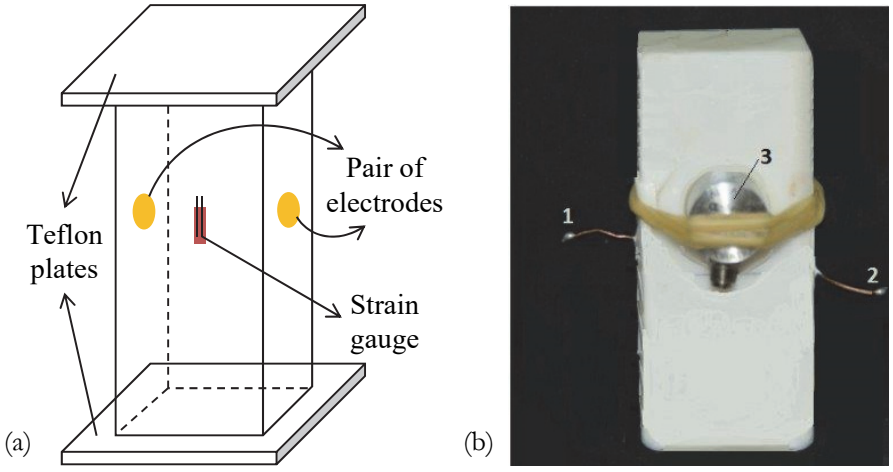

Figure 1: (a) A sketch of the experimental set up, (b) A typical marble specimen. The pair of electrodes (1, 2) and the acoustic sensor (3) are also presented.

RESULTS AND DISCUSSION

Mechanical behaviour

Typical stress-strain curves of each material are presented in Fig.2. The commonly observed "bedding error" during compressive tests is obvious in all three materials. Ignoring this initial part, the curves of both marble and cement mortar are mainly characterized by linearity up to about 80% of their maximum stress (points A and B in Fig.2a,b). The mean value of the fracture stress is ~95 MPa for marble and ~50 MPa for cement mortar. The modulus of elasticity obtained was equal to ~70 GPa and ~20 GPa for marble and mortar, respectively, which are very close to the respective ones from literature [10, 22]. Afterwards both curves deviate from linearity. On the other hand, the stress-strain curve of soda glass is linear almost up to 90% of the maximum stress of the specimens (point C in Fig.2c). Its modulus of elasticity was calculated equal to ~70 GPa as it is also mentioned in [31, 32] and its maximum stress was found to be equal to ~20 MPa. It is also to be noted that ductility of soda glass specimens is one order of magnitude lower than the respective ones of both marble and mortar. The mechanical characteristics obtained from all specimens are recapitulated in Tab. 2.

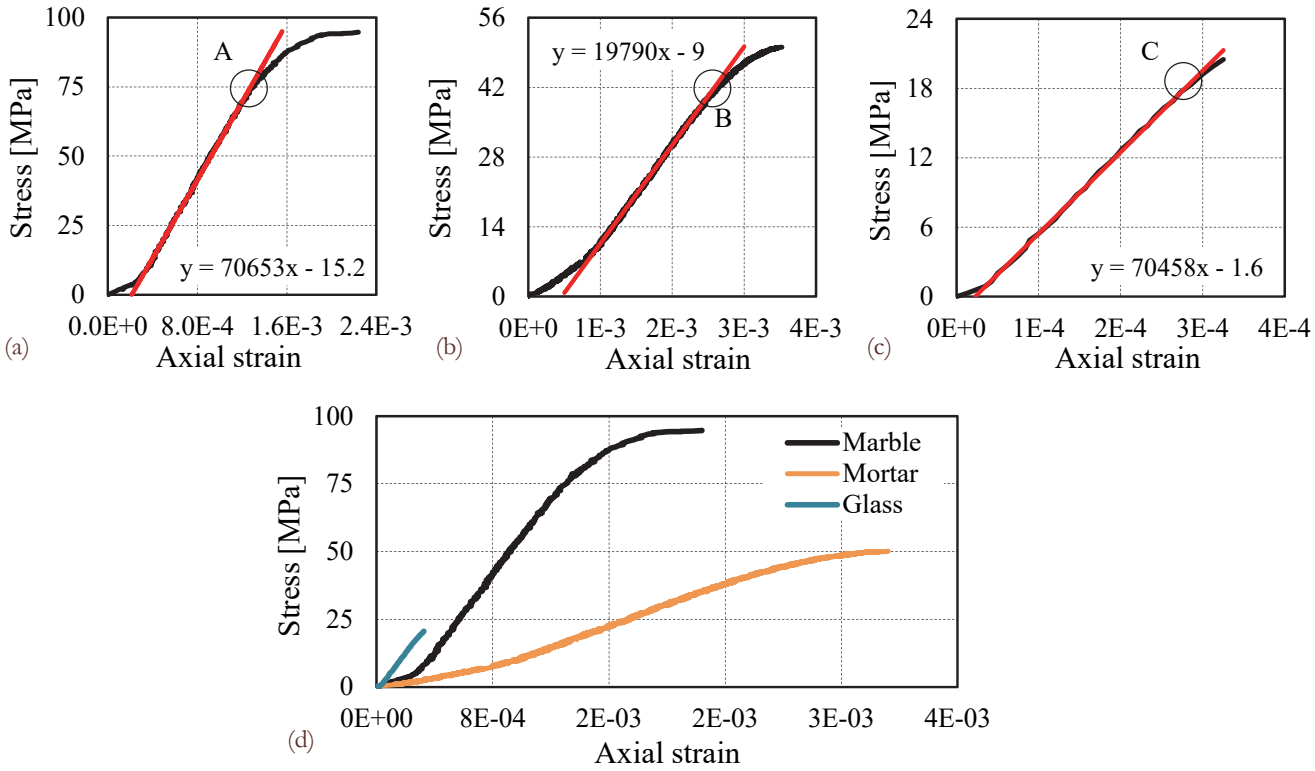

Figure 2: Typical stress-axial strain curves for (a) marble, (b) mortar and (c) glass specimens. (d) The three aforementioned curves together for comparison reasons.

Material	Specimen	Modulus of elasticity [GPa]	Fracture stress [MPa]	Peak axial strain [-]
Dionysos marble	M1	68.8	98.7	$1.7 \cdot 10^{-3}$
	M2	71.2	92.5	$1.9 \cdot 10^{-3}$
	M3	70.7	94.7	$2.2 \cdot 10^{-3}$
	Mean value ± standard deviation	70.2 ± 0.2	95.3 ± 0.5	$1.9 \cdot 10^{-3}$ ± 0.3
Cement mortar	C1	19.8	50.1	$3.5 \cdot 10^{-3}$
	C2	18.1	46.4	$2.4 \cdot 10^{-3}$
	C3	23.3	51.7	$3.1 \cdot 10^{-3}$
	Mean value ± standard deviation	20.4 ± 0.8	49.4 ± 0.5	$3.0 \cdot 10^{-3}$ ± 0.5
Soda glass	G1	68.7	18.8	$2.7 \cdot 10^{-4}$
	G2	70.5	20.5	$3.3 \cdot 10^{-4}$
	G3	70.0	19.4	$3.1 \cdot 10^{-4}$
	Mean value ± standard deviation	69.7 ± 0.2	19.6	$3.0 \cdot 10^{-4}$ ± 0.3

Table 2: The mechanical characteristics of all specimens.

Electric signals

The electric signal produced during a typical compressive test of a marble specimen and the axial strain obtained (normalized over its maximum value) versus the normalized stress are presented in Fig.3. A weak current (from 0.5 pA increases slightly to 2 pA) is initially observed until point A_1 in Fig.3(a1) where the stress level equals ~75% of the maximum stress and strain is ~55% of the fracture strain. This point almost corresponds to point A where the stress-strain curve

deviates from linearity. Afterwards, the electric current starts increasing with higher rate, indicating the onset of micro-cracking. When stress equals about 97% of the maximum applied stress (point A'$_1$ in Fig.3(a2) where the stress-strain curve tends to become horizontal) and strain equals about 80% of the maximum strain the increase of PSC is remarkable, severe cracking takes place (not yet visible with naked eyes) and the specimen is just before collapse.

In case of mortar specimens, the first noticeable change of the PSC values is observed when strain equals ~55% of the maximum strain and stress is ~60% of the maximum stress, point B$_1$ in Fig.3b) although the material is still below its proportional limit. The increase of the electric signal starts becoming significantly larger (point B'$_1$ in Fig.3b) when the respective stress-strain curve deviates from linearity (~75% of the maximum stress and ~70% of the fracture strain, point B in Fig.2b). PSC gets its maximum value slightly before the final fracture (~90% of the maximum strain and ~95% of the maximum stress) indicating the impending failure.

Concerning soda glass, the variation of PSC could be clearly divided in three stages. In the beginning of the test, a weak electric signal is detected until point C$_1$ in Fig.3c where strain is equal to ~60% of the maximum strain and stress is ~60% of the maximum stress. During the second stage (between points C$_1$ and C'$_1$ in Fig.3c), the increase of PSC is considerable while the increase rate becomes even higher during the last stage where the applied stress is ~85% of the maximum stress and strain equals ~80% of the maximum strain. The maximum value of PSC is attained ~96% of both the maximum stress and the maximum strain.

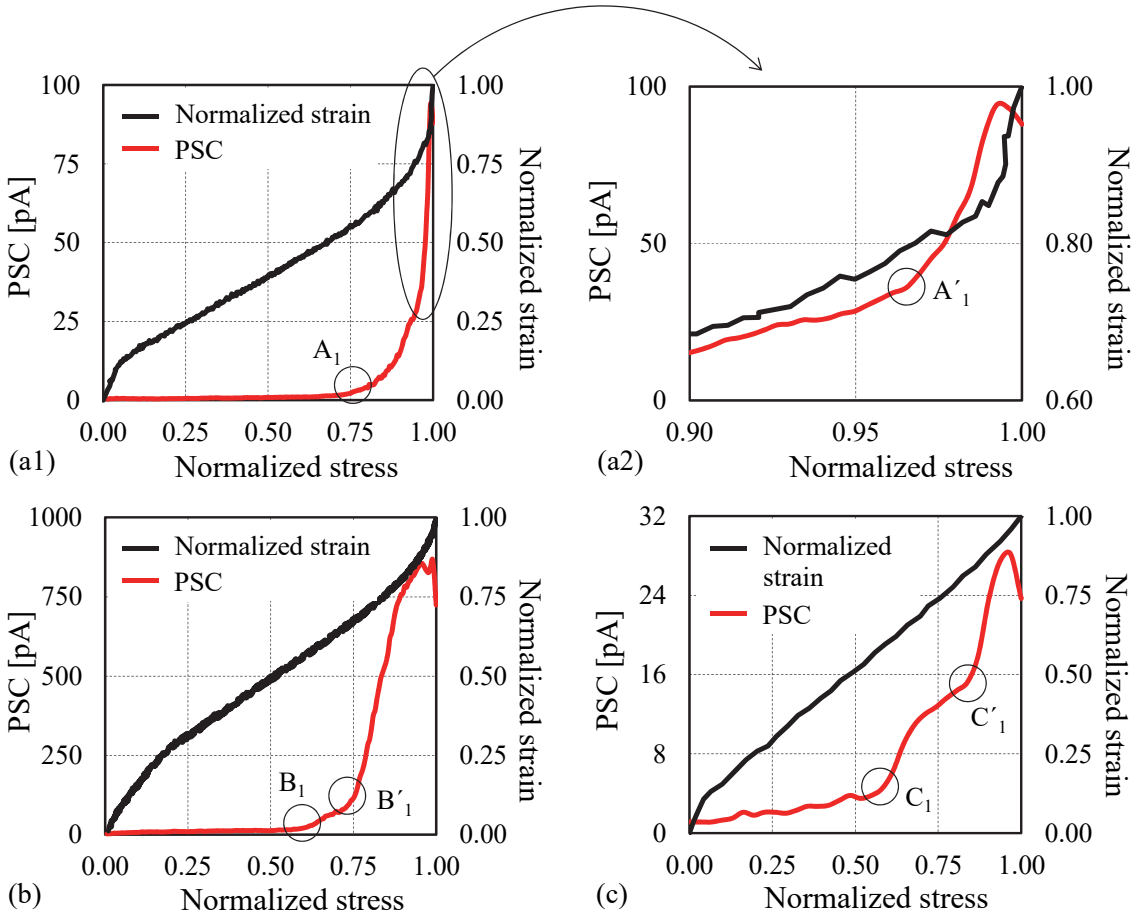

Figure 3: The electric current and the normalized axial strain versus the normalized stress for a typical specimen of (a) marble, (b) mortar and (c) glass.

PCS values in comparison with Ib-values

In all cases, groups of 70 hits were used for the calculation of the Ib-value. The first group included the first 70 hits while each successive group contained 35 hits of the previous one and the next 35 hits. Each Ib-value corresponds to the instant which was calculated as the mean time of the respective hits.

The variation of Ib-value in conjunction with the electric current is shown versus the normalized stress in Fig.4(a1) for a typical marble specimen. In the beginning of the test, until ~30% of the maximum strain and ~35% of the maximum

stress, Ib has high values decreasing from ~2.4 to 1.7. This can be related to the closure of pre-existing micro-cracks of the specimen or/and to rubbing/friction [1]. Afterwards, Ib-value is almost constant with variance around ~2.0 indicating the slow generation of new micro-cracks (until point A_2 in Fig.4(a1) which corresponds to stress level ~80% of the maximum stress and strain ~60% of the maximum strain). This point coincides with the deviation of the stress-strain curve from linearity. Slightly earlier, the first noticeable increase of the electric current was observed. Finally, Ib decreases systematically attaining at the end of the test values close to 1.0 (point A'_2 in Fig.4(a2)). This happens at ~95% of the maximum applied stress and ~75% of the maximum strain and it is related to a large number of cracks. During the decrease of Ib-value, PSC increases further. At the final stage (after point A'_2), Ib slightly decreases further due to the coalescence of cracks which leads the specimen to the final fracture while the electric current increases dramatically reaching its highest value.

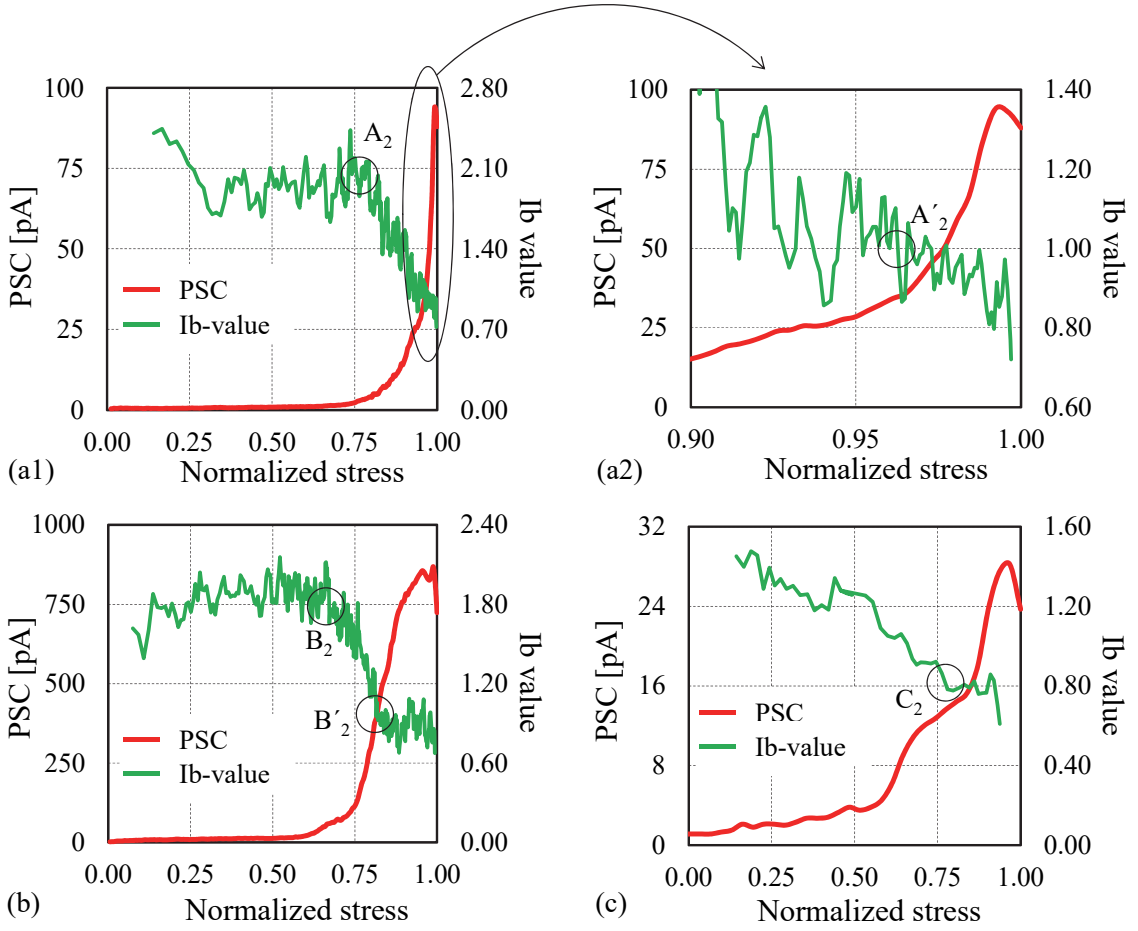

Figure 4: The electric current and the Ib-value against the normalized stress for a typical specimen of (a) marble, (b) mortar and (c) glass.

In case of mortar, Ib-value (Fig.4b) is relatively high from the beginning of the test until ~35% of both the maximum strain and the maximum stress while a period with almost constant Ib-value (~1.8) follows (until point B_2, ~60% of the maximum strain and ~70% of the maximum applied stress). Afterwards, Ib-value decreases (while the increase of PSC becomes significant) reaching the value of 1.0 (point B'_2) when the respective stress-strain curve ceases to be linear (~70% of the maximum strain and ~75% of the maximum stress). Subsequently, the values of Ib become slightly lower than 1.0 remaining almost constant until the fracture of the specimen. During this stage, the electric current attains its peak value indicating the impending failure.

The variation of the Ib-values for a typical soda glass specimen is presented in Fig.4c. Ib-value continuously decreases until point C_2 (~80% of both the maximum strain and the maximum stress), i.e. almost during the first two stages of the PSC variation. The rate of Ib-value decrease is higher between ~40% and ~80% of both the maximum strain and the maximum stress. Afterwards, Ib-value remains almost constant until ~90% of the maximum stress. From this point on and up to the end of the test, Ib-value decreases further. It is worth noticing that in case of soda glass, Ib-value attains the

value of 1.0 when strain is ~65% of the maximum strain and stress is ~65% of the maximum stress, i.e. relatively lower compared to the other two materials.
It should be mentioned at this point that b-value is related, among others, to the heterogeneity of the material. As the degree of nonuniformity of the material increases, b-value also increases [33]. This is consistent with the results of the present study. The material layers of marble and the existence of sand in mortar make these structures quite heterogeneous compared to glass specimens and as a result the Ib-values obtained for marble and mortar are larger than the respective values of glass. In addition, the heterogeneity of both marble and mortar results to the generation of low acoustic activity during the initial load levels leading to an almost constant Ib-value in these first stages of loading. The absence of this constant segment in case of glass makes the variation of the respective Ib-value to be monotonic in contrast to the respective variations of both marble and mortar.

Approach based on energies

Despite the fact that the correlation of PSC and AE techniques became clear in the previous section, an alternative approach based on the released energy was decided to be used in order to quantitatively verify the correlation of the two experimental techniques.
The absolute energy (measured in aJ) produced and recorded by the acoustic sensors characterizes each acoustic hit and it is calculated by the software as the integral of the signal voltage at a power of two over the reference resistance (10 kΩ). In the present study, the sum of the energy released during each second of the tests, E_{AE}, was calculated since it is a measure of the size distribution of micro-cracks in such materials [34]. In case of PSC technique, the energy released was calculated by the familiar expression:

$$E_{PSC}=\int_{t_i}^{t_i+\Delta t} PSC^2(t)dt \qquad (2)$$

where Δt=1 s and t_i= 0, 1, …, n-1 (n is the duration of the experiment). Since PSC is measured in pA, the units of E_{PSC} are $(pA)^2 \cdot s$. Finally, the strain energy density, SED, was calculated as the area below the stress-strain curves of the tests.
All three quantities were normalized over the respective maximum value and the results are presented in logarithmic scale in Fig.5. For all three materials of the present experimental protocol both curves are formed by two almost straight segments with different slope and a knee point is clearly seen corresponding probably to the formation of more severe cracks. In case of marble (Fig.5a), it is quite interesting that PSC technique seems to detect the internal damage of the specimen earlier than AE technique. In case of marble, the $PSC_{knee\ point}$ and the $AE_{knee\ point}$ correspond to about 70% and 80% of the maximum stress, respectively (i.e. about 50% and 60% of the maximum strain, respectively). The same is true for mortar specimens (Fig.5b). The knee point from PSC technique is observed when stress equals about 60% of the maximum stress (~55% of the maximum strain) while $AE_{knee\ point}$ corresponds to ~65% of the maximum stress and ~60% of the maximum strain. In case of glass specimens (Fig.5c), the knee points formed by the two techniques are observed almost simultaneously (~60% of both the maximum stress and strain).

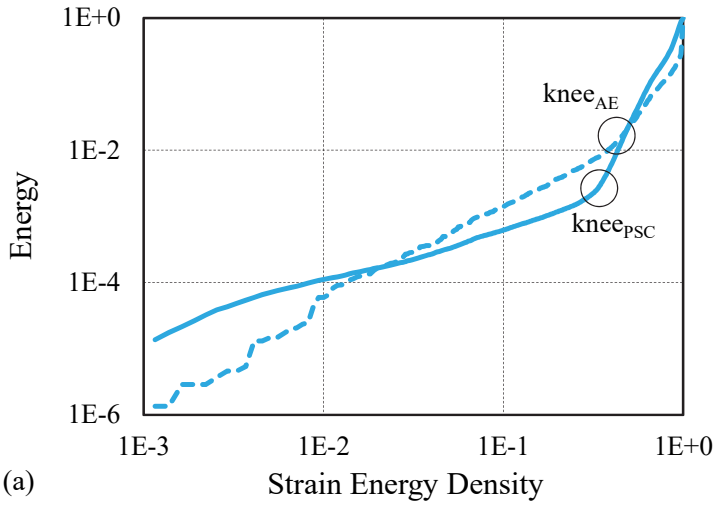

Figure 5: The energy calculated by both PSC and AE techniques versus the strain energy density for a typical specimen of (a) marble.

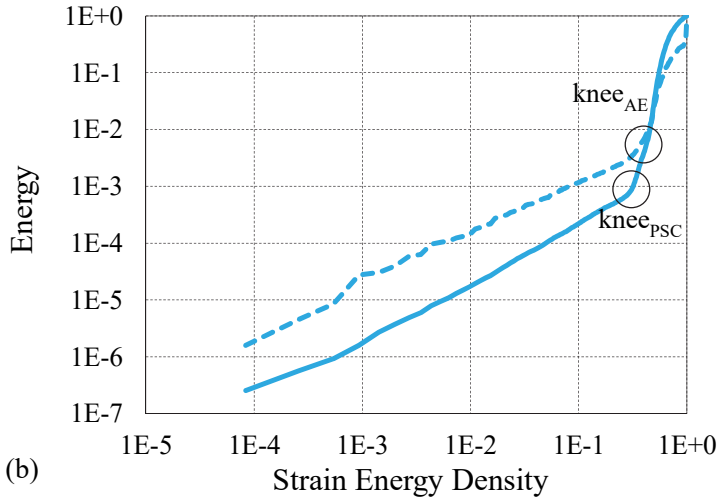

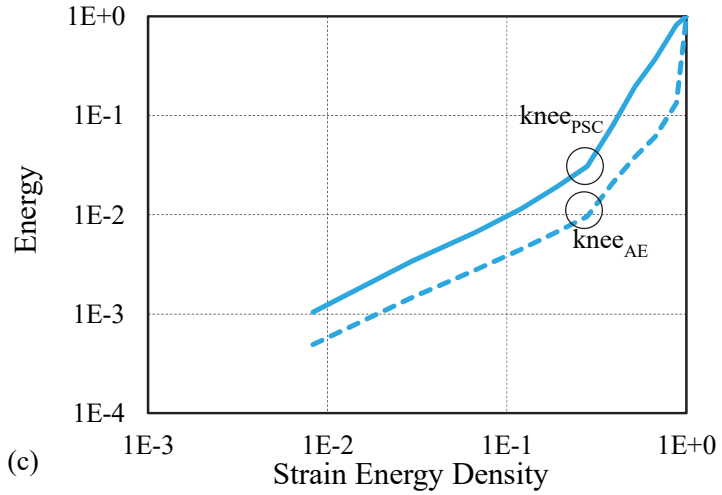

Figure 5 (con't): The energy calculated by both PSC and AE techniques versus the strain energy density for a typical specimen of (b) mortar and (c) glass.

As a next step, an effort was made to investigate any correlation which might exist between the quantities E_{PSC} and E_{AE} calculated by the two experimental techniques. In Figs.6(a-c) both energies are presented in logarithmic scale for a typical specimen for each material studied here. The solid dark blue circles represents the period where the electric current produced is very weak without noticeable changes while the empty symbols corresponds to the increase of the PSC until it reaches its maximum value. It is clear that the correlation is much better when the energy emitted increases considerably (empty dark blue circles). Therefore, ignoring the period where PSC is almost constant or increases very smoothly, it was found that the correlation of the energies calculated based on both experimental techniques obeys a power law, i.e. $E_{AE} \propto (E_{PSC})^m$, where m~0.8 for both marble and glass specimens while m~0.7 for mortar specimens (Figs.6(a-c)).

Conclusions

The correlation of both experimental techniques used in the present experimental protocol is highlighted. More specific, it was found that when the Ib-value decreases, the electric signal detected by the PSC technique starts increasing considerably indicating the formation of cracks. All three materials (marble, mortar and glass) enter a critical state (i.e. Ib-value tends to 1.0) when strain is equal to about 65-75% of the maximum strain (stress level equals to about 95% for marble, about 75% for mortar and about 65% for glass). The same stress level, at which the damage state of Dionysos marble becomes critical, is also obtained by other researchers based on the variation of the b-value [35].
The alternative approach which was based on the energy released during loading of the specimens, although it makes very

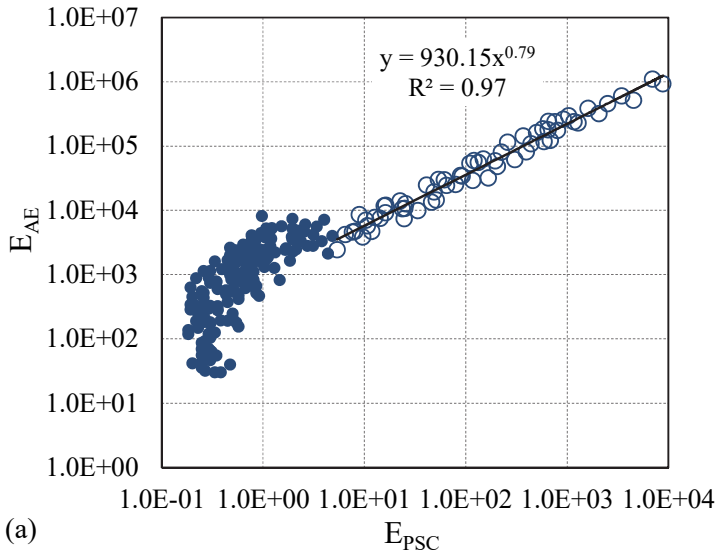

(a)

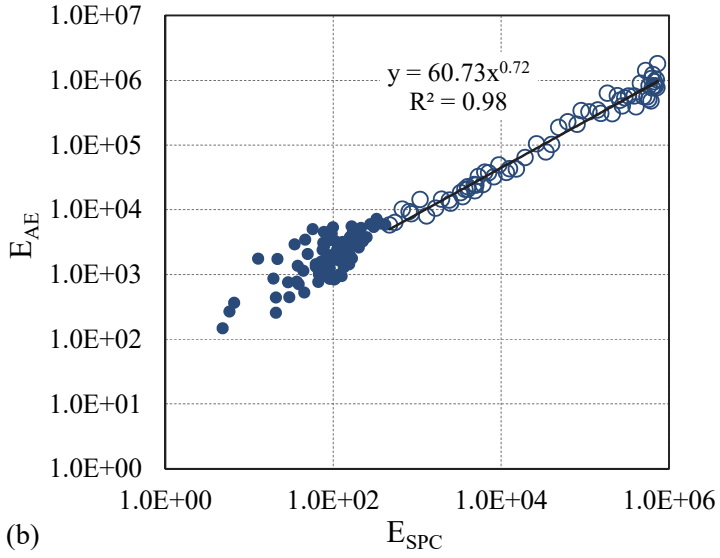

(b)

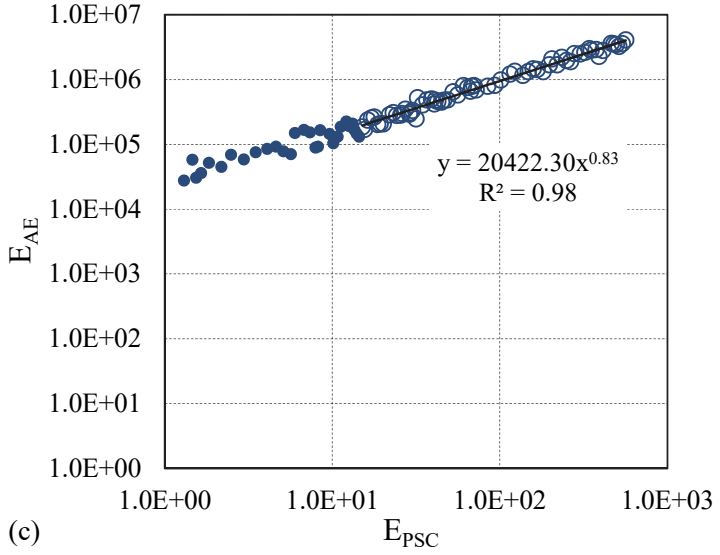

(c)

Figure 6: The correlation of the energy calculated by both PSC and AE techniques for a typical specimen of (a) marble, (b) mortar and (c) glass.

clear the point where cracking becomes more severe, it seems to be more conservative. The knee points are observed when strain equals about 50-60% of the fracture strain for all three materials studied here (while the stress level equals about 70-80% for marble specimens and about 55-65% for mortar and soda glass specimens).
AE technique has already been mentioned as a valuable tool for detecting the impending failure paying attention either to the general acoustic activity or to specific acoustic characteristics in accordance mainly to the stress induced on the specimens [18-19, 35-36].
PSC technique is more recently developed compared to the AE technique and it is not yet fully standardized. It should be mentioned that the specific technique cannot be applied in heavily distorted electromagnetic environments since very low electrical currents (in the order of pA) are measured and the external electrical noise acts as additive electrical noise on the actual signal. In order to minimize such effects special care must be given to the shielding of the experimental apparatus, electrical ground and low noise cabling. Despite the aforementioned limitations, the electric current recorded using the PSC technique has already been related to the mechanical behaviour of the tested material [4, 7].
Concluding, taking into account that strains are much easier to be measured, compared to the stress field developed, the fact that the critical state is detected by both techniques and it is determined at almost the same strain level for all three materials is an interesting finding which could be very useful for monitoring and assessing the integrity of structures.
In addition, in the direction of quantifying the correlation of the AE and the PSC techniques, a successful attempt is made for the very first time in the present paper. Indeed a very good correlation exists between the energies measured by both techniques, which obeys a power law with exponent equal to 0.7-0.8 for the materials studied here.

REFERENCES

[1] Rao, M.V.M.S., Lakschmi, P.K.J., Analysis of b-value and improved b-value of acoustic emissions accompanying rock fracture, Current Science, 89 (2005) 1577-1582.
[2] Colombo, S., Main, I.G., Forde, M.C., Assessing damage of reinforced concrete beam using "b-value" analysis of Acoustic Emission signals, Journal of Materials in Civil Engineering (ASCE), 15 (2003) 280-286.
[3] Shiotani, T., Yuyama S., Li, Z.W., Ohtsu, M., Application of the AE improved b-value to qualitative evaluation of fracture process in concrete materials, Journal of Acoustic Emission, 19 (2001) 118-132.
[4] Stavrakas, I., Triantis, D., Agioutantis, Z., Maurigiannakis, S., Saltas, V., Vallianatos, F., Pressure Stimulated Currents in rocks and their correlations with mechanical properties, Natural Hazards and Earth System Sciences, 4 (2004) 563-567.
[5] Enomoto, J., Hashimoto, H., Emission of charged particles from indentation fracture of rocks, Nature, 346 (1990) 641-643.
[6] Vallianatos, F., Triantis, D., Tzanis, A., Anastasiadis, C., Stavrakas, I., Electric earthquake precursors: From laboratory results to field observations, Physics and Chemistry of the Earth, 29 (2004) 339-351.
[7] Triantis, D., Anastasiadis, C., Vallianatos, F., Kyriazis, P., Nover, G., Electric signal emissions during repeated abrupt uniaxial compressional stress steps in amphibolite from KTB drilling, Natural Hazards and Earth System Sciences, 7 (2007) 149-154.
[8] Vallianatos, F., Triantis, D., Scaling in Pressure Stimulated Currents related with rock fracture, Physica A, 387 (2008) 4940-4946.
[9] Triantis, D., Anastasiadis, C., Stavrakas, I., The correlation of electrical charge with strain on stressed rock samples, Natural Hazards and Earth System Sciences, 8 (2008) 1243-1248.
[10] Kyriazopoulos, A., Anastasiadis, C., Triantis, D., Brown, C.J., Non-destructive evaluation of cement-based materials from pressure-stimulated electrical emission - Preliminary results, Construction and Building Materials, 25 (2011) 1980-1990.
[11] Aydin, A., Prance, R.J., Prance, H., Harland, C.J., Observation of pressure stimulated voltages in rocks using an electric potential sensor, Applied Physics Letters, 95 (2009) art no. 124102.
[12] Freund, F., Pre-earthquake signals: Underlying physical processes, Journal of Asian Earth Sciences, 41 (2011) 383-400.
[13] Cartwright-Taylor, A., Vallianatos, F., Sammonds, P., Superstatistical view of stress-induced electric current fluctuations in rocks, Physica A: Statistical Mechanics and its Applications, 414 (2014) 368-377.
[14] Li, Z., Wang, E., He, M., Laboratory studies of electric current generated during fracture of coal and rock in rock burst coal mine, Journal of Mining, 2015 (2015) article ID 235636.
[15] Archer, J.W., Dobbs, M.R., Aydin, A., Reeves, H.J., Prance, R.J., Measurement and correlation of acoustic emissions and pressure stimulated voltages in rock using an electric potential sensor, International Journal of Rock Mechanics and Mining Sciences, 89 (2016) 26-33.

[16] Dann, D., Demikhova, A., Fursa, T., Kuimova, M., Research of electrical response communication parameters on the pulse mechanical impact with the stress–strain state of concrete under uniaxial compression, IOP Conference Series: Materials Science and Engineering, 66(1) (2014) 012036, doi:10.1088/1757-899X/66/1/012036
[17] Stergiopoulos, C., Stavrakas, I., Hloupis, G., Triantis, D., Vallianatos, F., Electrical and Acoustic Emissions in cement mortar beams subjected to mechanical loading up to fracture, Engineering Failure Analysis, 35 (2013) 454–461.
[18] Stavrakas, I., Pasiou, E.D., Hloupis, G., Malliaros, G.-T., Triantis, D., Kourkoulis, S.K., Exploring the size effect of marble by combined use of Pressure Stimulated Currents and Acoustic Emission, in: Beskos D.E., Stavroulakis G.E. (Eds.), 10th HSTAM International Congress on Mechanics, Chania, Hellas, (2013) 185-186.
[19] Triantis, D., Stavrakas, I., Pasiou, E.D., Hloupis, G., Kourkoulis, S.K., Innovative experimental techniques in the service of restoration of stone monuments - Part II: Marble epistyles under shear, Procedia Engineering, 109C (2015) 276-284.
[20] Tassogiannopoulos, A.G., A contribution to the study of the properties of structural natural stones of Greece (in Greek), Ph.D. Dissertation, National Technical University of Athens, Greece (1986).
[21] Theocaris, P.S., Coroneos, E., Experimental study of the stability of Parthenon, Publications of the Academy of Athens, 44 (1979) 1-80.
[22] Kourkoulis, S.K., Exadaktylos, G.E., Vardoulakis I., U-notched Dionysos-Pentelicon marble in three point bending: The effect of nonlinearity, anisotropy and microstructure, International Journal of Fracture, 98(3-4) (1999) 369-392.
[23] Kourkoulis, S.K., Ganniari-Papageorgiou, E., Mentzini, M., Dionysos marble under bending: A contribution towards understanding the fracture of the Parthenon architraves, Engineering Geology, 115 (3-4) (2010) 246-256.
[24] Exadaktylos, G.E., Vardoulakis, I., Kourkoulis, S.K., Influence of nonlinearity and double elasticity on flexure of rock beams - I. Technical theory, International Journal of Solids and Structures, 38 (22-23) (2001) 4091-4117.
[25] Exadaktylos, G.E., Vardoulakis, I., Kourkoulis, S.K., Influence of nonlinearity and double elasticity on flexure of rock beams - II. Characterization of Dionysos marble, International Journal of Solids and Structures, 38 (22-23), (2001) 4119-4145.
[26] Exadaktylos, G.E., Kaklis, K.N., Applications of an explicit solution of the transversely isotropic circular disc compressed diametrically, International Journal of Rock Mechanics and Mining Sciences, 38(2) (2001) 227-243.
[27] Markides, Ch.F., Pazis, D.N., Kourkoulis, S.K, Influence of friction on the stress field of the Brazilian tensile test, Rock Mechanics and Rock Engineering, 44(1) (2011) 113-119.
[28] Markides, Ch.F., Kourkoulis, S.K., The stress field in a standardized Brazilian disc: The influence of the loading type acting on the actual contact length, Rock Mechanics and Rock Engineering, 45(2) (2012) 145-158.
[29] Kourkoulis, S.K., Prassianakis, I., Agioutantis, Z., Exadaktylos, G.E., Reliability assessment of the NDT results for the internal damage of marble specimens, International Journal of Material and Product Technology, 26(1/2) (2006) 35-56.
[30] Kosmatka, S.H., Kerkhoff, B., Panarese, W.C., Design and control of concrete mixtures (14th ed.), Portland Cement Association (2002).
[31] Chorfa, A., Madjoubi, M.A., Hamidouche, M., Bouras, N., Rubio, J., Rubio, F., Glass hardness and elastic modulus determination by nanoindentation using displacement and energy methods, Ceramics - Silikáty, 54(3) (2010) 225-234.
[32] Sehgal, J., Ito, S., Brittleness of glass, Journal of Non-Crystalline Solids, 253 (1999) 126-132.
[33] Mogi, K., Earthquakes and fractures, Tectonophysics, 5(1) (1967) 35-55.
[34] Rao, M.V.M.S., Lakshmi K.J.P., Rao, G.M.N., Vijayakumar, K., Udayakumar, S., Precursory microcracking and brittle failure of Latur basalt and migmatite gneiss under compressive loading, Current Science, 101(8) (2011) 1053-1059.
[35] Nomikos, P.P., Sakkas, K.M., Sofianos, A.I., Acoustic emission of Dionysos marble specimens in uniaxial compression, Harmonising Rock Engineering and the Environment, Qian and Zhou (eds.), Taylor & Francis Group, London, ISBN 978-0-415-80444-8.
[36] Agioutantis, Z., Kaklis, K., Mavriagiannakis, S., Verigakis, M., Vallianatos, F., Saltas, V., Potential of acoustic emissions from three point bending tests as rock failure precursors, International Journal of Mining Science and Technology, 26 (2016) 155-160.